Design of InP Segmented-collector DHBTs with Reduced Collector Transit Time τ_c for Large Power Bandwidth Power Amplifiers

Yihao Fang[1], Jonathan P. Sculley[2], Miguel E Urteaga[3], Andy D Carter[3], Paul D. Yoder[2], and Mark J. W. Rodwell[1]
[1]*Department of Electrical and Computer Engineering, University of California, Santa Barbara, 93106, USA*
[2]*School of Electrical and Computer Engineering, Georgia Institute of Technology, Atlanta, 30332, USA*
[3] *Teledyne Scientific and Imaging, 1049 Camino Dos Rios, Thousand Oaks, CA, 91360, USA*
Email: yihaofang@ece.ucsb.edu / Phone: (424) 208-9822

InP double-heterojunction bipolar transistors (DHBTs) have demonstrated power gain cutoff frequencies (f_{max}) above 1THz under low collector voltage due to electron velocity overshoot in the InP drift collector [1][2]. Under higher collector voltage, however, a quick onset of Γ-L scattering limits the average electron velocity to the saturation velocity (**Fig. 1 (a)-(c)**), leading to a Johnson's figure-of-merit (JFOM) second to GaN HEMTs and a limited transistor power bandwidth for InP DHBTs [3]. Here we propose a *velocity-engineered* device structure called the segmented-collector DHBT (SC-DHBT) that incorporates p-type scattering layers within the drift collector to reduce the electron kinetic energy and force a greater electron distribution into the low effective mass Γ-valley for extended velocity overshoot (**Fig. 3 (a)**). Transport simulations show the collector transit time τ_c is reduced from 1.23ps in the reference design to 0.90ps in a double scatterer design at V_{cb} = 5V, J_c = 1mA/um^2. The proposed SC-DHBT design is suited for large power bandwidth power amplifiers.

The proposed segmented-collector structure includes a single or double 30nm p++-InGaAs scatterer layers in a baseline 300nm InP drift collector. Γ-L scattering is suppressed by intentional inelastic collisions between mobile electrons and local holes confined by valence band offsets in the scatterers (**Fig. 2 (a)-(b)**). Electrons exiting the p++ scatterers relax to the Γ-valley edge as ~30nm corresponds to the energy mean free path for electrons in p++-InGaAs [4]. Therefore, these electrons can accelerate again in Γ-valley to the overshot velocity, leading to an average velocity higher than the saturation velocity through the drift collector (**Fig. 3 (b)-(c)**). Two important results of the full band ensemble Monte Carlo simulations done at Georgia Tech are: 1). electron velocity within the p++ InGaAs scatterers is ~3×10^7cm/s *regardless of* V_{cb}, which is in agreement with empirical p++-InGaAs base transit time measured by UCSB and Teledyne; and 2). Γ-L scattering occurs almost precisely when electrons injected from the base gain a kinetic energy E_k of 0.7eV, again, *regardless of* V_{cb}. To expedite device epi-structure design, a numerical self-consistent velocity-field solver has been developed at UCSB based on the Georgia Tech results to optimize the placement of scatterers. Electrons entering the drift collector are assumed to accelerate ballistically from the Γ-valley edge if E_k < 0.7eV. The resultant electron velocity is calculated with nonparabolicity corrections [5]. If $E_k \geq$ 0.7eV, electron velocity is pinned at a saturation velocity of 9×10^6cm/s (**Fig. 1 (c)**). Electron velocity within the p++-InGaAs scatterers is set constant at 3×10^7cm/s. Electrons leaving the scatterers accelerate ballistically again until $E_k \geq$ 0.7eV (**Fig. 2 (b)**). At a given J_c and V_{cb}, the local electron density and its associated current-induced band bending are calculated and made self-consistent with the velocity profile after iterations. Collector transit time $\tau_c = \partial Q_b / \partial I_c$ as a function of J_c and V_{cb} is, then, calculated per Shockley-Ramo theorem [6], as such definition of τ_c can be readily utilized in C_π in InP DHBTs' RF small-signal model. τ_c of the *baseline* 300nm collector as a function of J_c and V_{cb} is plotted in **Fig. 4**. τ_c with *single* p++ scatterer inserted at *Position* = 70nm is plotted in **Fig. 5**. τ_c with *double* p++ scatterers inserted at *Position* = 60nm & 160nm is plotted in **Fig. 6**. Significant bias-dependent τ_c dispersion is observed for the baseline design, whereas segmented collector designs are affected to a lesser degree, especially under low bias conditions. A hybrid-π small-signal model is used to provide a qualitative measure of linearity of the different collector designs (**Fig. 7**). Under 4V < V_{cb} < 6V, 0 < J_c < 2mA/um^2, f_T of the baseline collector is between 80GHz and 125GHz; f_T of the 70nm insertion single scatterer collector is between 90GHz and 120GHz; and f_T of the 60nm & 160nm insertion double scatterer collector is between 100GHz and 130GHz. Reduction in velocity modulation, therefore, also improves transistor linearity.

[1] M Urteaga, *et al*, DRC, Santa Barbara, CA, 2011 [2] K Kurishima, *et al*, Jpn. J. Appl. Phys. vol. 31, pt. 2 no. 6b Jun 1992 [3] K Shinohara, *et al*, IEEE TED vol. 60, no. 10 Oct 2013 [4] T Kaneto, et al, Appl. Phys. Lett. vol. 63, no. 48 Jul 1993 [5] V Ariel-Altschul, *et al*, IEEE TED vol. 39, no. 6 Jun 1992 [6] W. Shockley, J. Appl. Phys. vol. 9 pp. 635 Oct 1938

978-1-5386-3028-0/18/$31.00 ©2018 IEEE

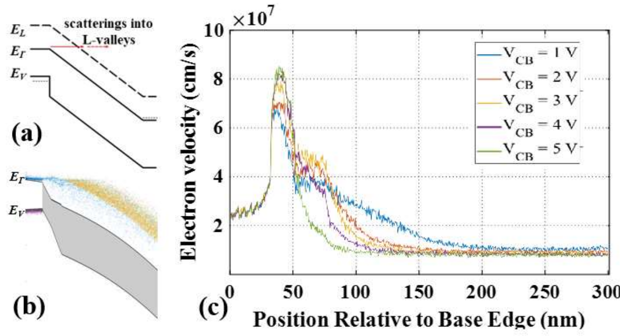

Fig. 1: **(a)** Schematic of Γ-L scattering and region of velocity overshoot; **(b)** Georgia Tech Monte Carlo simulation result for 300nm thick InP collector (V_{cb} = 2V, J_c = 0.5mA/um^2), electrons in Γ-valley are blue, L-valleys yellow; **(c)** Simulated electron velocity as a function of V_{cb} with constant J_c = 0.5mA/um^2.

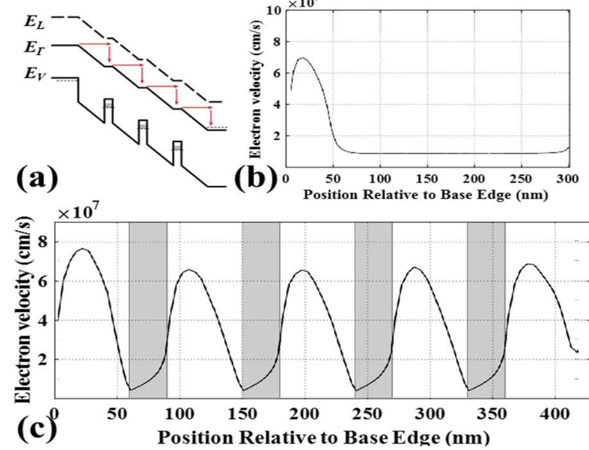

Fig. 3: **(a)** Schematic of the SC-DHBT and inelastic relaxation of electrons to Γ-valley edge; **(b)** Electron velocity profile for a uniform 300nm collector (V_{cb} = 5V, J_c = 0mA/um^2); **(c)** Electron velocity vs. position for a 400nm segmented collector with four p++-InGaAs scatterers under the same bias conditions.

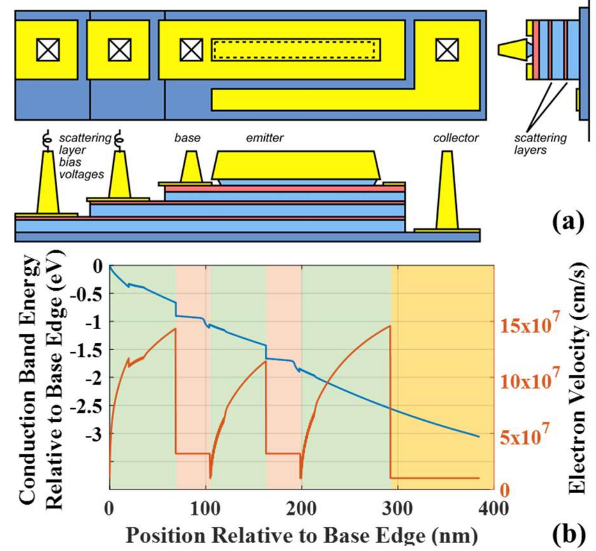

Fig. 2: **(a)** Schematics of the segmented-collector DHBT with p++ scatterer layers inserted in the drift collector region. The scatterers are biased with AC chokes to control band bending in the drift collector; **(b)** Example of conduction band profile and electron velocity profile of a double scatterer drift collector simulated by UCSB numerical solver (V_{cb} = 2V, J_c = 0.005mA/um^2). Green = ballistic acceleration; red = diffusive transport in p++ scatterers; orange = velocity saturation due to Γ-L scattering.

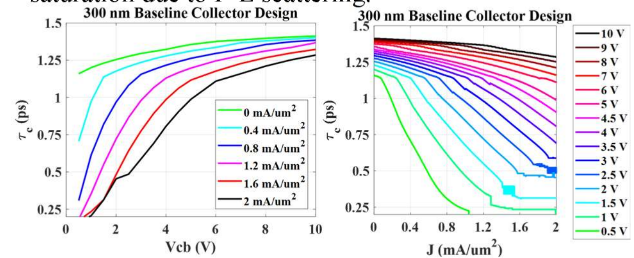

Fig. 4: τ_c as a function of voltage (left), and of current (right) for the uniform 300nm baseline collector.

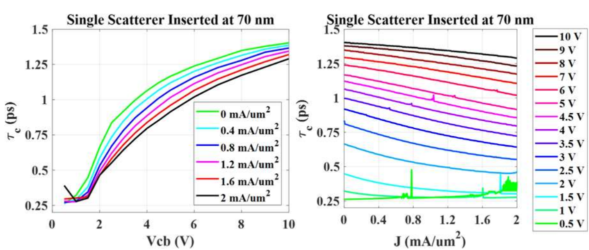

Fig. 5: τ_c as a function of voltage (left), and of current (right) for a single scatterer inserted at *Position* = 70nm.

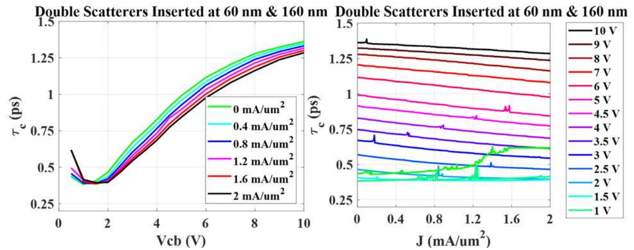

Fig. 6: τ_c as a function of voltage (left), and of current (right) for double scatterers inserted at *Position* = 60nm & 160nm.

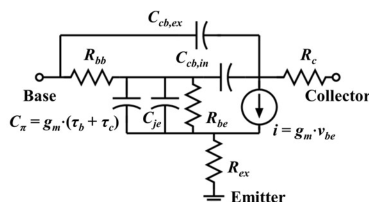

Fig. 7: A hybrid-π equivalent model for extraction of f_T with $C_{cb,ex}$ = 2.5fF, R_{bb} = 26Ω, $C_{cb,in}$ = 0.83fF, R_c = 4Ω, $C_\pi = g_m \cdot (\tau_b + \tau_c)$, τ_b = 110fs, $g_m = k_B T/(A_E \cdot J_c)$, A_E = 1um^2, C_{je} = 15fF, R_{be} =170Ω, R_{ex} = 6Ω.

978-1-5386-3028-0/18/$31.00 ©2018 IEEE